

# Superconductivity in metal coated graphene

B. Uchoa\*, and A. H. Castro Neto

Physics Department, Boston University, 590 Commonwealth Ave., Boston, MA 02215

We show that graphene, a single atomic layer of graphite, can become a superconductor when coated with a dilute layer of alkali metal. We propose a microscopic mechanism of superconductivity based on the attraction of electrons in graphene mediated by a screened acoustic plasmon of the metal. We discuss the phase diagram for superconductivity in graphene, which has two different singlet superconducting phases: with symmetry  $s$  and  $p + ip$  wave.

Graphite intercalated compounds (GIC) with alkali or rare-earth metals such as  $\text{NaC}_2$ ,  $\text{YbC}_6$ , and  $\text{CaC}_6$  show superconductivity with unprecedented high critical temperatures for graphite-based compounds [1, 2], although neither pure graphite nor alkali metals superconduct in ordinary conditions [3]. So far, the highest critical temperature obtained in GIC is  $T_c \sim 11.5$  K for  $\text{CaC}_6$ . Similar behavior has been observed in  $\text{C}_{60}$  fullerenes doped with very diluted concentrations of alkali metals, which superconduct at temperatures as high as 30 K [4, 5]. We show that the recently discovered graphene [6], which consists of a single atomic layer of graphite and is the carbon matrix for GIC and fullerenes, can become a superconductor when coated with a diluted layer of alkali metal.

A common characteristic of all superconducting GIC is the occupation of a three dimensional (3D) interlayer band of nearly free electrons, and in parallel, the transfer of electrons from the metal to the  $\pi$ -bands of graphite. For instance, Li is a good donor in graphite, but its electrons do not occupy the interlayer band, except in high Li concentrations:  $\text{LiC}_6$  and  $\text{LiC}_3$  have empty interlayer bands and do not superconduct, while the compound  $\text{LiC}_2$  has the interlayer band weakly occupied and superconducts at  $T_c \sim 1.9$  K [7, 8]. These experimental facts indicate that the superconductivity in GIC should be described by a two-band model.

On general grounds, superconductivity can be expected from an interaction between electrons and a collective mode, producing a retarded attractive interaction (as in the case of the electron-phonon coupling in ordinary superconductors). One of a few known purely electronic mechanisms that can produce superconductivity is due to the interaction of electrons with acoustic plasmons, the collective modes of a Fermi sea. This mechanism has been widely considered for two-band models in metals [9] and oxides [10].

The 3D character of the interlayer band in GIC generated skepticism in regards to the plasmon mechanism since the 3D plasmons are optical in nature. However, electronic screening can convert the 3D optical plasmon into an acoustic mode, as originally proposed by Fröhlich in the context of the two-band superconductivity model [11]. A similar mechanism based on screened acoustic plasmons is theoretically possible in GIC. In alkali coated graphene this mechanism of pairing is very effective because of the high velocity of its electrons, and also due to the presence of an additional unscreened acoustic plasmon, that strongly reduces the Coulomb repulsion.

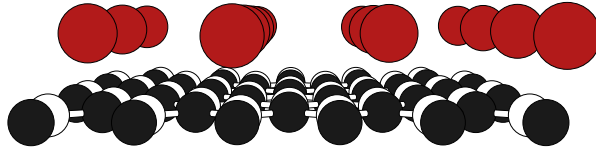
Although there is controversy on the role of the optical phonons to the strong superconductivity shown in  $\text{CaC}_6$  [12], in Ca coated graphene optical phonons should not play a role since the Ca ions form a triangular lattice with one atom per unit cell (the interaction between the Ca and C atoms is rather weak and should not affect the optical phonon spectrum), as we show in Fig. 1, leading to a single acoustic phonon mode. Since the sound velocity of the ions is  $\sim 10^4$  times smaller than the electron velocity, the acoustic phonons are much less effective than the acoustic plasmons in mediating Cooper pairing, implying that the superconductivity of Ca coated graphene can be purely electronic. We propose that electrons in graphene attract each other via a screened acoustic plasmon of the metal. We show that this mechanism is favorable to superconductivity when the metal is sufficiently dilute. We also discuss the mean-field phase diagram, where two different singlet superconducting phases arise:  $s$ -wave and  $p + ip$  pairing.

The Hamiltonian of the graphene-metal system can be written as:  $H = H_t + H_g + H_m + H_{m-g}$ , where,

$$H_t = -\mu \sum_i \hat{n}_{g,i} - t \sum_{\langle ij \rangle} \sum_{s=\uparrow\downarrow} (a_{i,s}^\dagger b_{j,s} + h.c.), \quad (1)$$

is the non-interacting graphene Hamiltonian associated with the electronic hopping between nearest neighbors C atoms of the honeycomb lattice.  $t \approx 2.7$  eV is the hopping energy,  $a_{i,s}$  ( $a_{i,s}^\dagger$ ) is the on-site annihilation (creation) operator for electrons in the sublattice  $A$  with spin  $s = \uparrow, \downarrow$ , and  $b_{i,s}$  ( $b_{i,s}^\dagger$ ) for sublattice  $B$ ,  $\hat{n}_{g,i}$  is the on-site particle density operator, and  $\mu$  is the graphene chemical potential (we use units such that  $\hbar = 1 = k_B$ ). Diagonalization of (1) leads to a spectrum given by:  $\epsilon_{\mathbf{k}} = -t|\gamma_{\mathbf{k}}|$ , where  $\mathbf{k}$  is the two-dimensional (2D) momentum, and  $\gamma_{\mathbf{k}} = \sum_{\vec{\delta}} e^{i\mathbf{k} \cdot \vec{\delta}}$  ( $\vec{\delta}_1 = a(\hat{x}/2 + \sqrt{3}/2\hat{y})$ ,  $\vec{\delta}_2 = a(\hat{x}/2 - \sqrt{3}/2\hat{y})$ , and  $\vec{\delta}_3 = -a\hat{x}$ , where  $a \approx 1.42$  Å is the C-C distance). As in graphite,

a



b

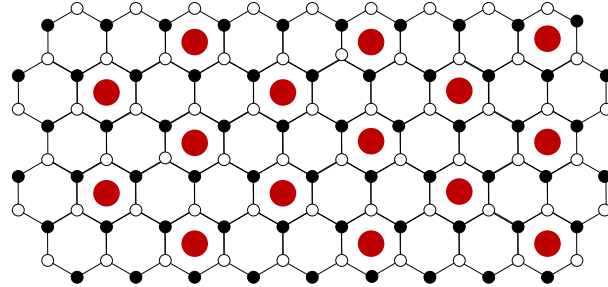


FIG. 1: **Graphene coated with metallic atoms.** (a) The carbon atoms in the two different sublattices are represented in black and white, and the metallic atoms are shown in red. (b) Top view of the atoms for  $[MC_6]_{2D}$  where M is the metal.

the unique electronic properties of pure graphene sheet are due to the fact that the spectrum is linear in  $\mathbf{k}$  around the corners of the hexagonal Brillouin zone (at  $\mathbf{Q}_0 = [2\pi/(3a), 2\pi(3\sqrt{3}a)]$  and symmetric points), where the band has the shape of a Dirac cone:  $\varepsilon_{\mathbf{Q}_0+\mathbf{k}} = \pm v_0 |\mathbf{k}|$ , with  $v_0 = 3at/2 \approx 6$  eV Å is the Fermi-Dirac velocity. In neutral graphene (in the absence of the metal layer and applied gate voltages), the chemical potential crosses exactly through the Dirac point, where the electronic density of states vanishes, leading to its many unusual properties [13]. When the alkali metal is deposited on top of the graphene lattice, the metal electrons migrate to the  $\pi$ -band, raising up the chemical potential from the Dirac points and lowering the energy of the nearly free electron band (NFE) of the metal to the Fermi level in order to restore the electrostatic equilibrium. Electron-electron interactions in graphene are described by the Hamiltonian,

$$H_g = \sum_{ij} V(\mathbf{R}_i - \mathbf{R}_j) \hat{n}_{g,i} \hat{n}_{g,j} \quad (2)$$

where  $\mathbf{R}_i$  labels the  $i^{\text{th}}$  site of the graphene layer, and  $V(\mathbf{r}) = e^2/(\epsilon_0 |\mathbf{r}|)$  is the Coulomb potential ( $e$  is the electron charge and  $\epsilon_0 \approx 2.4$  is the background dielectric constant [14]). As noted previously [15], the relative strength of the Coulomb interactions to the kinetic energy in neutral graphene is determined by graphene's dimensionless fine structure constant,  $\alpha_g = e^2/v_0 \approx 2$ .

The normal metal electrons are described by the Hamiltonian:

$$H_m = \sum_{s,\mathbf{k}} (\epsilon_{\mathbf{k}} - E_F) f_{\mathbf{k}s}^\dagger f_{\mathbf{k}s} + \sum_{ij} V(\mathbf{r}_i - \mathbf{r}_j) \hat{n}_f(\mathbf{r}_i) \hat{n}_f(\mathbf{r}_j), \quad (3)$$

where  $\epsilon_{\mathbf{k}} = k^2/(2m)$  is the free particle dispersion ( $m$  is the electron mass), and  $\hat{n}_f(\mathbf{r}_j) = \sum_s f_s^\dagger(\mathbf{r}_j) f_s(\mathbf{r}_j)$ , where  $\mathbf{r}_j$  labels the  $j^{\text{th}}$  site of the metal layer, is the particle density operator. The Fermi energy of the 2D metal can be written as:  $E_F = mv_F^2/2 = r_s^{-2}/(ma_0^2) \approx 25r_s^{-2}$  eV, where  $v_F = k_F/m$  is the Fermi velocity ( $k_F = \sqrt{2\pi\sigma}$  is the Fermi momentum, where  $\sigma$  is the number of electrons per unit of area in the metal),  $a_0 = 1/(me^2) \approx 0.53$  Å is Bohr radius, and the dimensionless quantity  $r_s = e^2/(\sqrt{\pi\sigma}/m) = 1/(a_0\sqrt{\pi\sigma})$ , measures the relative strength of Coulomb interaction to the kinetic energy in the metal.

Finally,  $H_{m-g}$  is the Coulomb interaction between electrons of the metal and the graphene layer,

$$H_{m-g} = 2 \sum_{ij} V(\mathbf{r}_i - \mathbf{R}_j) \hat{n}_f(\mathbf{r}_i) \hat{n}_{g,j}. \quad (4)$$

Notice that we have assumed that there is no direct hopping between the metal and graphene, and that electrons in each material only interact through Coulomb forces. This assumption is based on the chemistry of the system:

the electro-negativities of a metal atom and Carbon are so different that, once the charge transfer between the two layers is finished, the electronic wavefunctions become localized in each layer. This assumption is in agreement with *ab initio* calculations for K adsorbed in graphene at low metal coverages [16].

The presence of the Coulomb interaction between layers (4) induces an effective electron-electron interaction for electrons in the graphene layer that can be calculated with the use of the random phase approximation (RPA) [17]. The diagrammatic RPA expansion in terms of the zeroth order polarization functions of the metal,  $\Pi_m^0$ , and of graphene,  $\Pi_g^0$ , results in an effective *retarded* interaction of the form (see section Methods):

$$H_{\text{eff}}^g = \sum_{\mathbf{q}} \sum_{\omega} V_{\text{eff}}(\mathbf{q}, \omega) \hat{n}_g(\mathbf{q}, \omega) \hat{n}_g(-\mathbf{q}, -\omega), \quad (5)$$

where,

$$V_{\text{eff}}(\mathbf{q}, \omega) = \frac{V_{0,q}}{\epsilon_T(\mathbf{q}, \omega)} [1 - (V_{0,\mathbf{q}} - V_{d,\mathbf{q}}) \Pi_m^0(\mathbf{q}, \omega)], \quad (6)$$

is the effective electron-electron interaction,

$$\epsilon_T(\mathbf{k}, \omega) = 1 - V_{0,q} [\Pi_g^0(\mathbf{k}, \omega) + \Pi_m^0(\mathbf{k}, \omega)] + (V_{0,q}^2 - V_{d,q}^2) \Pi_m^0(\mathbf{k}, \omega) \Pi_g^0(\mathbf{k}, \omega), \quad (7)$$

is the total dielectric function of the system, and

$$V_{d,\mathbf{q}} = 2\pi e^2 e^{-qd}/(\epsilon_0 q) \quad (8)$$

is the Fourier transform of the Coulomb interaction between electrons in two layers separated by a distance  $d$ . In eq. (7) the separation between the metal and the graphene layer induces an additional crossed polarization term, that vanishes when  $d = 0$ . In the opposite limit,  $kd \gg 1$ , the two layers decouple. In this last case, the total dielectric function is simply the product of the graphene and the metal dielectric functions,  $\epsilon_T(\mathbf{k}, \omega) = \epsilon_g(\mathbf{k}, \omega) \epsilon_m(\mathbf{k}, \omega)$ , and the effective interaction (6) becomes the expected result for pure graphene (namely,  $V_{0,q}/\epsilon_g(\mathbf{q}, \omega)$ ).

The main observation about eq. (6) is that the effective interaction changes from repulsive to attractive as a function of frequency (see Fig. 2 (b)). In fact, the dielectric function (7) vanishes at the plasmon frequency  $\Omega_p(q)$  ( $\epsilon_T(q, \Omega_p) = 0$ ), and hence for frequencies smaller (larger) than  $\Omega_p(q)$  the interaction is attractive (repulsive). When  $qd \ll 1$  and  $|\omega| \ll v_0 q$ , the plasmon behaves as a collective mode of the metal screened by the electrons of graphene. It has a linear dispersion,  $\Omega_p(q) \approx \sqrt{E_F^*/(2\mu)} v_0 q$ , where  $E_F^* = E_F [1 + (8e^2 d \mu / \epsilon_0 v_0^2)]$  is the Fermi energy of the metal renormalized by the effect of the spacing between the two layers. For  $qd \gg 1$ , the plasmon is not screened, and one recovers the plasmon dispersion for the 2D electron gas:  $\Omega_p \rightarrow \Omega_m = e\sqrt{2E_F q / \epsilon_0} \propto \sqrt{q}$ . In the region  $v_F q < |\omega| \ll v_0 q$ , eq. (6) can be approximated as:

$$V_{\text{eff}}^g(q, |\omega| \ll v_0 q) = \frac{V_{0,q}}{\epsilon_g(q, 0)} \left[ \frac{\Omega_p^2 - (1 - e^{-qd}) \Omega_m^2}{\omega^2 - \Omega_p^2} + 1 \right]. \quad (9)$$

The interaction (9) is strongly attractive for  $|\omega| \lesssim \Omega_p(q)$ , inside the region 1 in Fig. 2 (a). Near the plasmon frequency, the electrons of graphene resonate with the screened collective modes of the metal, opening up the possibility for creation of superconducting pairs. In this attractive region, the graphene electrons are sufficiently fast to screen charge fluctuations and restore the longitudinal response of the graphene collective modes in the normal phase, that is required to preserve the local gauge invariance of the superconductor [18]. The electrons of the metal, by their turn, are too slow to screen efficiently any charge imbalance. As shown by the Eliashberg calculation of Garland [19] for transition metals with a nearly free *s*-band and a narrow *d* electron band, the slow electrons of the *d*-band tend to anti-screen the fast *s* electrons. The final result is an average repulsive interaction among the *d* electrons, in contrast to the *s* electrons, which superconduct. In a two-band system of graphene and a metal the situation is inverted: the Dirac fermions in graphene are fast and can resonate with the collective modes of the slow electrons of the metal, which do not superconduct.

In the high frequency limit  $|\omega| \gg v_0 q$ , the effective interaction (6) has a second region of attraction (region 2 of Fig. 2 (a)). For  $qd \ll 1$ , the effective interaction in this region can be approximated by

$$V_{\text{eff}}^g(q, |\omega| \gg v_0 q) = V_{0,q} \left[ \frac{\Omega_{2D}^2}{\omega^2 - \Omega_{2D}^2} + 1 \right]. \quad (10)$$

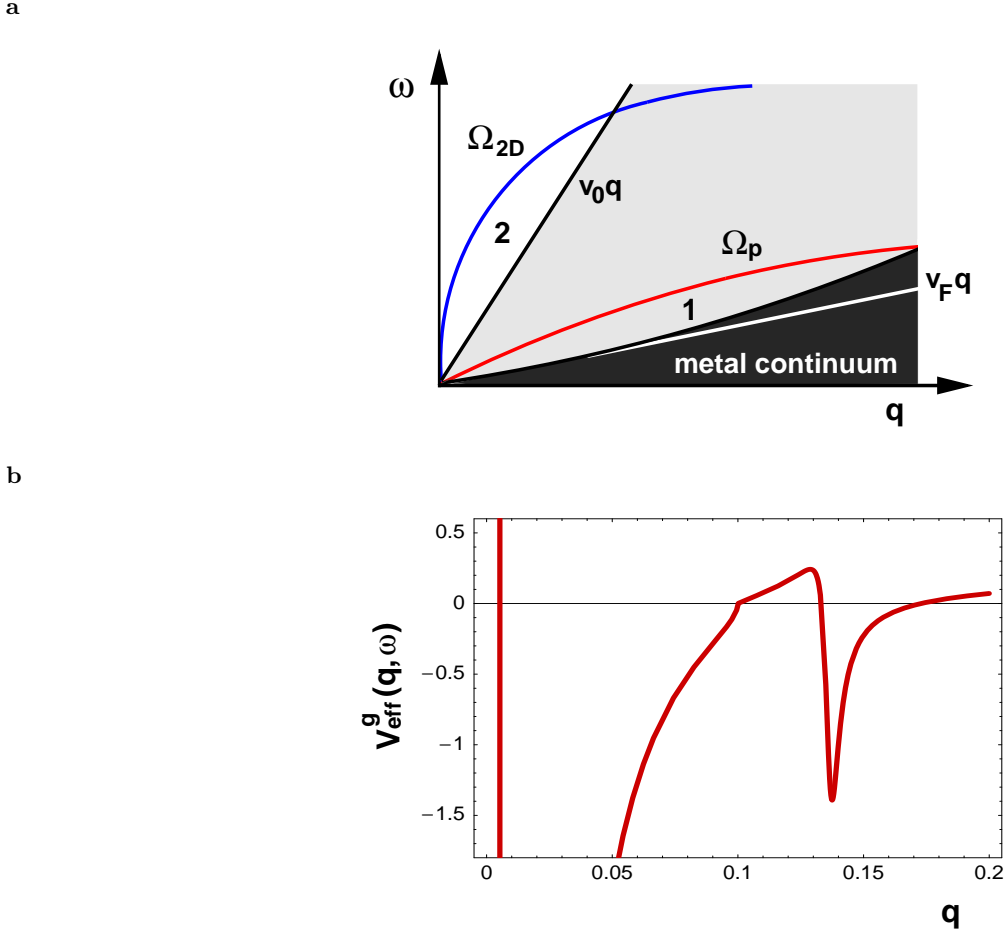


FIG. 2: **Effective electron-electron interaction** (a) Frequency,  $\omega$ , versus momentum,  $q$ , diagram with the excitations in the metal-graphene system. The dark and grey regions are the particle-hole continuum of the metal and of graphene, respectively. The dispersion of the screened plasmon mode,  $\Omega_p(q)$  goes to zero linearly with  $q$ . The second mode,  $\Omega_{2D}$  is the unscreened plasmon characteristic of the 2D electron gas. The effective interaction between electrons in graphene is attractive in regions 1 and 2. (b) Effective interaction (in units of  $63 \text{ eV } \text{\AA}^2$ ) as a function of  $q$  (in units of  $\mu/v_0$ ) for  $\omega = 0.1\mu$ , induced by the metallic coating ( $E_F \approx 0.4 \text{ eV}$  and  $\mu \approx 3 \text{ eV}$ ).

where  $\Omega_{2D}(q) = e\sqrt{2(E_F + \mu)q/\epsilon_0}$  is a plasmon mode originating from all electrons. This plasmon has the usual dispersion for a plasmon in the 2D electron gas. We note that the interaction (10) is attractive for  $|\omega| < \Omega_{2D}(q)$ . This attractive region, however, is present in the ordinary 2D electron gas, and does not lead itself to superconductivity, although it favors the formation of a superconductor ground state by reducing the Coulomb repulsion.

Therefore, a necessary condition for the appearance of superconductivity in coated graphene is that the screened acoustic plasmon is not overdamped by the electronic particle-hole continuum. This mode is defined in the interval  $v_F q < \Omega_p \ll v_0 q$ . In the long wavelength limit,  $qd \ll 1$ , the condition for the existence of this acoustic mode is:

$$E_F \ll 2\mu\epsilon_0/(\epsilon_0 + 8\alpha_g d\mu/v_0) < mv_0^2/2, \quad (11)$$

where  $mv_0^2/2 \approx 2.4 \text{ eV}$  indicating that superconductivity is possible if  $r_s \gtrsim r_{s,\min} \approx 3.2$  in order to assure that the screened plasmon is well defined outside the particle-hole continuum of the metal, as shown in Fig. 2 (a). The left hand side of the inequality in eq. (11) assures that the acoustic plasmons are slower than the Dirac fermions, which are allowed to screen. For large  $\mu$ , the second term in inequality (11) saturates and we may write this inequality as:

$$E_F \ll \epsilon_0 v_0 / (4d\alpha_g). \quad (12)$$

Assuming [20]  $d \sim 2 \text{ \AA}$  the inequality is obeyed if  $E_F \ll 0.9 \text{ eV}$ , which is equivalent to the condition that  $r_s \gg r_{s,\min} \approx 5$ . This condition implies that the electronic concentration in the metal layer has to be smaller than  $\sigma_c \approx 4 \times 10^{14}$

electrons  $\text{cm}^{-2}$  (or 0.12 electrons per C). We also note that superconductivity should disappear at very low electron densities (see below) because the screened plasmon frequency decreases with decreasing density, and the attractive region in the effective potential (6) shrinks. Thus, there is an optimal electron concentration for the observation of superconductivity in the system.

Hence, there must be a maximum (minimum) metal concentration above (below) which superconductivity is not possible. Each metal atom donates  $y$  electrons to graphene [16, 20]. At very low metal concentrations  $y$  is just the atomic valence,  $v$ , of the metal but as the metal density increases, the charging energy of the graphene plane also increases, and the electron transfer is halted when the charging energy becomes roughly of the order of the difference in energy between the atomic energies of the metal atom and C. Therefore, the number of remaining electrons per atom in the metal layer,  $x = v - y$ , is a function of the metal density, and has to be calculated from first principles [20, 21]. For a system with chemical composition [22]  $[\text{M}_n \text{C}_m]_{2D}$  where M is the metal atom and  $n, m$  are integers (we assume the metal lattice to be commensurate with graphene), there will be  $(n/m)y$  electrons in each carbon. Thus, one of the conditions for superconductivity is that:

$$x \ll 0.12(m/n). \quad (13)$$

This result predicts that  $[\text{CaC}_6]_{2D}$  ( $n = 1, m = 6$ ), as shown in Fig. 1, should superconduct for  $x \ll 0.7$ . These estimates indicate that graphene may become a superconductor for a sufficiently low metallic coverage. Values of  $x$  of this order are obtained in K adsorbed in graphite [16].

Alkali metal adsorption on graphite is an active field of research [16], and it is possible to obtain metallic superstructures even at very low metal concentrations. Potassium, K, has been used for this purpose, and a monolayer (i.e.,  $[\text{KC}_8]_{2D}$  with  $4.8 \times 10^{14}$  atoms  $\text{cm}^{-2}$ ), or even a small fraction of a monolayer (i.e.,  $[\text{KC}_{98}]_{2D}$  with  $3.9 \times 10^{13}$  atoms  $\text{cm}^{-2}$ ), can be produced at liquid Nitrogen temperatures. Low density K coverage in graphite show a disperse K phase with gigantic spacing between K atoms of  $\sim 60 \text{ \AA}$  [20]. A somehow similar behavior was observed in other alkali metals like Rb and Cs [16], indicating that other alkali atoms in graphite might be able to form a stable homogeneous lattice or at least a homogeneously distributed phase with a well defined mean spacing between the atoms at very low concentrations.

To estimate the critical temperature through a BCS-like calculation, the retarded interaction (9) is replaced by a static step function potential  $V_{\text{app.}}(\omega) = -U_0 \theta(\Lambda_0 - \omega)$ . Here,  $\Lambda_0 = v_F q_0$  is the cut-off calculated at the energy where the acoustic plasmon intercepts the metal particle-hole continuum, and  $U_0$  is the effective strength of the interaction. This kind of estimate is not accurate because eq. (9) indicates that the attractive interaction goes to strong coupling for small momentum  $q$ , since electrons and screened acoustic plasmons have comparable energy scales and couple strongly. In strong coupling, small uncertainties on  $U_0$  affect drastically the BCS estimates of the critical temperature, and a more rigorous microscopic calculation of  $T_c$  must include explicitly the retarded interaction [21].

However, the physics of the problem can be understood qualitatively by a simple phenomenological model. We start from the effective Hamiltonian of graphene, after the electrons of the metal have been traced out, including on-site and inter-sublattice interactions:

$$\begin{aligned} H_{\text{eff}}^g = & -t \sum_s \sum_{\langle ij \rangle} a_{is}^\dagger b_{js} + \text{h.c.} - \mu \sum_{is} [a_{is}^\dagger a_{is} + b_{is}^\dagger b_{is}] + \frac{g_0}{2} \sum_{is} [a_{is}^\dagger a_{is} a_{i-s}^\dagger a_{i-s} + b_{is}^\dagger b_{is} b_{i-s}^\dagger b_{i-s}] \\ & + g_1 \sum_{\langle ij \rangle} \sum_{s,s'} a_{is}^\dagger a_{is} b_{js'}^\dagger b_{js'}, \end{aligned} \quad (14)$$

where  $g_0$  and  $g_1$  are the on-site and nearest neighbor electron-electron interaction energies, respectively, induced by the metal layer, eq. (9). The condensation of the graphene electrons into Cooper pairs can occur in two principal channels: (1)  $s$ -wave pairing,

$$\Delta_0 = \langle a_{i\downarrow} a_{i\uparrow} \rangle = \langle b_{i\downarrow} b_{i\uparrow} \rangle; \quad (15)$$

(2) spin singlets between electrons in different sub-lattices,

$$\Delta_{1,ij} = \langle a_{i\downarrow} b_{j\uparrow} - a_{i\uparrow} b_{j\downarrow} \rangle. \quad (16)$$

We assume the simplifying *ansatz*, where  $\Delta_{1,ij} = \Delta_1$  for all nearest neighbors and zero otherwise. In the reciprocal space, the symmetry of  $\Delta_{1,ij}$  is driven by the band symmetry of the  $\pi$  carbon orbitals,

$$\Delta_{\mathbf{k}} = \sum_{ij} \Delta_{1,ij} e^{-i\mathbf{k} \cdot (\mathbf{r}_i - \mathbf{r}_j)} = \Delta_1 \gamma_{\mathbf{k}}^*.$$

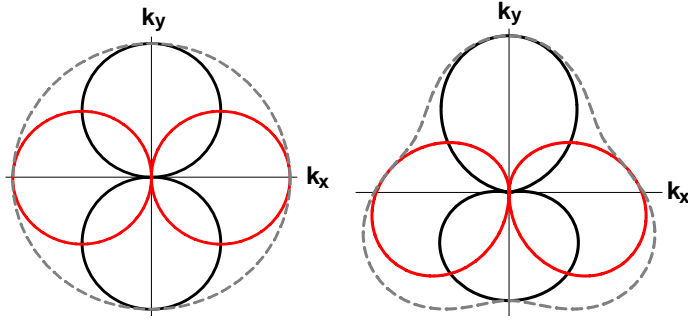


FIG. 3: **Superconducting gap in the  $p + ip$  state.** Real (black) and imaginary (red) parts of the order parameter,  $\Delta_{\mathbf{k}} = \Delta_1 \gamma_{\mathbf{k}}^*$ , calculated around the Dirac points at low (left) and large (right) electron concentrations. The dashed line shows the total amplitude of the order parameter,  $|\Delta_{\mathbf{k}}|$ .

Close to the Dirac points  $\mathbf{Q}_0$ , the non-local order parameter has the momentum dependence:  $\Delta_{\mathbf{Q}_0 + \mathbf{k}} = (3/2)\Delta_1(k_y + ik_x)$ , which describes a  $p + ip$ -wave order parameter (see Fig. 3). Notice, surprisingly, that although the state has  $p + ip$  symmetry, it is still a singlet because of the sub-lattice structure of the honeycomb lattice.

The problem can be analyzed at the mean-field level and one finds three distinct phases (see section Methods): *i*) an  $s$ -wave phase for  $g_0 < 0$  and  $g_1 > 0$ , *ii*) a  $p + ip$ -wave phase for  $g_0 > 0$  and  $g_1 < 0$ , and *iii*) a phase with mixed symmetry for  $g_0, g_1 < 0$ . The two superconductor transitions, normal to  $s$ -wave and normal to  $p + ip$ -wave, defined in terms of the interaction parameters  $g_0$  and  $g_1$  are continuous, but the transitions involving the mixed phase for  $g_0 < 0$  and  $g_1 \rightarrow 0$  or  $g_1 < 0$  and  $g_0 \rightarrow 0$  are of first-order even at  $T = 0$ . At the critical temperature,  $T_c$ , the phase transitions of phases *i* and *ii* to the normal state are second order, while the transition between the mixed phase and the normal phase is abrupt. The phenomenology of the  $s$ -wave phase for Dirac fermions can be understood in the context of nodal liquid superconductivity [23]. In the weak coupling limit, i.e. for  $g_0 \ll g_c = 2\pi v_0^2/\Lambda$ , where  $\Lambda$  is a high energy cut-off, the critical temperature is given by:

$$T_c \approx 2\mu(\gamma/\pi)e^{-\Lambda(g_c/g_0-1)\mu^{-1}-1}, \quad (17)$$

where  $\ln \gamma \sim 0.577$ . In accordance with previous discussion, eq. (17) shows that  $T_c$  goes to zero at low electron (metal) densities ( $\mu \rightarrow 0$ ) and vanishes in pure graphene.

In reality, however, because the system is 2D there can be no true superconducting long-range order (Mermin-Wagner theorem) but there will be a Kosterlitz-Thouless (KT) transition below a certain temperature  $T_{KT} < T_c$ . Hence,  $T_c$  only establishes the temperature below which the amplitude of the order parameter becomes finite while its phase still fluctuates. Phase coherence only occurs at low temperatures and depends on the phase stiffness of the system. Although the transition is of the KT type, one expects a precipitous drop of the resistivity of the material below  $T_{KT}$  indicating the entrance of the electrons into a state of quasi-long-range superconducting order.

In summary, we have proposed that metal coated graphene can be made superconducting through a screened acoustic plasmon mechanism, when the metallic density is low. We have set the bounds for the observation of superconductivity and studied its phase diagram that contains both  $s$ -wave, as well as,  $p + ip$  pairing. Our results indicate that superconductivity can be quite robust in this system. Our proposal open new doors for the study of graphene based systems, that became a reality since their discovery just a few years ago [6].

## Methods

### Polarization functions

The electronic susceptibility of the NFEB,  $\Pi_m^0$ , is described by the 2D Lindhard polarization function. When  $\omega > v_F q$ , the  $q \rightarrow 0$  limit of the Lindhard function gives [17]:

$$V_{0,q}\Pi_m^0(q, \omega) = \Omega_m^2/\omega^2, \quad (18)$$

where  $\Omega_m(q) = e\sqrt{2E_F q/\epsilon_0}$  is the acoustic plasmon of the 2D electron gas ( $\epsilon_m(\mathbf{q}, \Omega_m) = 0$ ). The polarization function of graphene at small momentum  $q$  is dominated by intra-band excitations, involving processes connecting states in

the same branch of the Dirac cone [14]:

$$\Pi_g^0(q, \omega) = -(2\mu/\pi v_0^2) \left[ 1 - \omega/\sqrt{\omega^2 - v_0^2 q^2} \right]. \quad (19)$$

In the low frequency limit,  $\omega \ll v_0 q$ , the polarization function of graphene is approximated by its static part,  $\Pi_g^0(q, 0)$ , and the total dielectric function (7) becomes:

$$\epsilon_T(q, \omega) = \epsilon_g(q, 0) \left[ 1 - \Omega_p^2(q)/\omega^2 \right], \quad (20)$$

where,

$$\Omega_p^2(q) = (\Omega_m^2(q)/\epsilon_g(q, 0)) \left[ 1 - (1 - e^{-2qd}) V_{0,q} \Pi_g^0(q, 0) \right], \quad (21)$$

is the screened plasmon mode of the metal, defined as the zero of the total dielectric function (7).

In the high frequency limit,  $|\omega| \gg v_0 q$ , the polarization function of graphene (19) gives

$$V_{0,q} \Pi_g^0(q, \omega) = \Omega_g^2/\omega^2, \quad (22)$$

where  $\Omega_g(q) = e\sqrt{2\mu q/\epsilon_0}$  is the acoustic plasmon of pure graphene. For  $qd \ll 1$  and  $|\omega| \gg v_0 q$ , the total dielectric function (7) becomes:

$$\epsilon_T(q, \omega) = \left[ 1 - \Omega_{2D}^2(q)/\omega^2 \right], \quad (23)$$

where  $\Omega_{2D}(q) = \sqrt{\Omega_g^2(q) + \Omega_m^2(q)}$  is the unscreened plasmon frequency.

### Mean-field theory

Decoupling the quartic terms in eq. (14) at the mean-field level we find:

$$H_P = g_0 \Delta_0 \sum_i (a_{i\uparrow}^\dagger a_{i\downarrow}^\dagger + b_{i\uparrow}^\dagger b_{i\downarrow}^\dagger) + \text{h.c.} + g_1 \sum_{\langle ij \rangle} \Delta_{1,ij} (a_{i\uparrow}^\dagger b_{j\downarrow}^\dagger - a_{i\downarrow}^\dagger b_{j\uparrow}^\dagger) + \text{h.c.} - g_0 \sum_i \Delta_0^2 - \sum_{\langle ij \rangle} g_1 \Delta_{1,ij}^2. \quad (24)$$

The total Hamiltonian can be diagonalized into the form:  $H_{eff}^g = \sum_{\mathbf{k}} \sum_{\alpha} \omega_{\mathbf{k}\alpha} \hat{n}_{\mathbf{k},\alpha}^B + E_0$ , where  $E_0 = -g_0 \Delta_0^2 - 3g_1 \Delta_1^2$ , and  $\hat{n}_{\mathbf{k},\alpha}^B$  is the quasi-particle density operator of the new fermions indexed by the four branches,  $\alpha = 1, \dots, 4$ , of the spectrum:  $\omega_{\mathbf{k},\alpha} \equiv \pm \omega_{\mathbf{k},s}$ , where

$$\omega_{\mathbf{k},s} = \sqrt{(t|\gamma_{\mathbf{k}}| + s\mu)^2 + (g_0 \Delta_0 + sg_1 \Delta_1 |\gamma_{\mathbf{k}}|)^2}, \quad (25)$$

with  $s = \pm 1$  labeling the two particle-hole branches.

The values of  $\Delta_0$  and  $\Delta_1$  are calculated from the minimization of the free energy:

$$F = -\frac{1}{\beta} \sum_{\alpha=1}^4 \sum_{\mathbf{k}} \ln (1 + e^{-\beta \omega_{\mathbf{k}\alpha}}) + E_0,$$

where  $\beta = 1/T$ . The coupled self-consistent equations for the gaps are:

$$\Delta_0 = -\frac{1}{2} \sum_{\mathbf{k}} \sum_{s=\pm 1} \frac{\tanh(\beta \omega_{\mathbf{k}s}/2)}{\omega_{\mathbf{k}s}} [g_0 \Delta_0 + s |\gamma_{\mathbf{k}}| g_1 \Delta_1], \quad (26)$$

$$\Delta_1 = -\frac{1}{6} \sum_{\mathbf{k}} \sum_{s=\pm 1} \frac{\tanh(\beta \omega_{\mathbf{k}s}/2)}{\omega_{\mathbf{k}s}} |\gamma_{\mathbf{k}}| [g_1 \Delta_1 |\gamma_{\mathbf{k}}| + sg_0 \Delta_0]. \quad (27)$$

- 
- [1] Belash, I. T., Bronnikov, A. D., Zharikov, O. V., Palnichenko, A. V., On the superconductivity of graphite intercalation compounds with sodium. *Solid State Commun.* **64**, 1445-1447 (1987).
- [2] Weller, T. E., Ellerby, M. E., Saxena, S. S., Smith, R. P., Skipper, N. T. Superconductivity in the intercalated graphite compounds  $C_6Yb$  and  $C_6Ca$ . *Nat. Phys.* **1**, 39-41 (2005).
- [3] Jishi, R. A., Dresselhaus, M. S., Superconductivity in graphite intercalation compounds, *Phys. Rev. B* **45**, 12465 (1992).
- [4] Hebard, A. F. *et. al.*, Superconductivity at 18 K in potassium-doped  $C_{60}$ , *Nature* **352**, 223-225 (1991).
- [5] Kelty, P. S., Chen, C.-C., & Lieber, C. M. Superconductivity at 30 K in caesium-doped  $C_{60}$ , *Nature* **350**, 600-601 (1991).
- [6] Novoselov, K. S. *et al.* Electric field effect in atomically thin carbon films, *Science* **306**, 666-669 (2004).
- [7] Csanyi, G. C., Littlewood, P. B., Nevidomskyy, Pickard, C. J., Simons, B. D., The role of the interlayer state in the electronic structure of superconducting graphite intercalate compounds, *Nat. Phys.* **1**, 42-45 (2005).
- [8] Belash, I. T., Bronnikov, A. D., Zharikov, O. V., Palnichenko, A. V., Superconductivity of graphite intercalation compound with lithium  $C_2Li$ . *Solid State Commun.* **69**, 921-923 (1989).
- [9] Richardson, C. F., Ashcroft, N. W., Effective electron-electron interactions and the theory of superconductivity, *Phys. Rev. B* **55**, 15130 (1997).
- [10] Ruvalds, J., Plasmons and high-temperature superconductivity in alloys of copper oxides, *Phys. Rev. B* **35**, 8869-8872 (1987).
- [11] Fröhlich, H., Superconductivity in metals with incomplete inner shells, *J. Phys. C* **1**, 544-548 (1968).
- [12] Mazin, I. I., Unresolved problems in superconductivity of  $CaC_6$ , *cond-mat/0606404*.
- [13] Peres, N. M. R., Guinea, F., and Castro Neto, A. H., Electronic properties of disordered two-dimensional carbon, *Phys. Rev. B* **73**, 125411 (2006).
- [14] Shung, K. W.-K., Dielectric function and plasmon structure of stage-1 intercalated graphite, *Phys. Rev. B* **34**, 979-993 (1986).
- [15] Peres, N. M. R., Guinea, F., and Castro Neto, A. H., Coulomb interactions and ferromagnetism in pure and doped graphene, *Phys. Rev. B* **72**, 174406 (2005).
- [16] For a review, see Caragiu, M., Finberg, S., Alkali metal adsorption on graphite: a review, *J. Phys.: Condens. Matter* **17**, R995-R1024 (2005), and references therein.
- [17] Fetter, A. L., Walecka, J. D., *Quantum theory of many-particle systems*. (McGraw-Hill, New York, 1971)
- [18] Pines, D., and Schrieffer, J.R., Gauge invariance in the theory of superconductivity, *Nuovo Cimento* **10**, 496 (1958).
- [19] Garland, J. M. Mechanisms for superconductivity in the transition metals, *Phys. Rev. Lett.* **11**, 111 (1963).
- [20] Lamoen, D., B. N. J. Persson, Adsorption of potassium and oxygen on graphite: a theoretical study, *Journal of Chem. Phys.* **108**, 3332 (1998).
- [21] Uchoa, B., and Castro Neto, A. H., in preparation.
- [22] We use the notation  $[M_nC_m]_{2D}$  in order to distinguish these systems from their 3D GIC counterparts that have the same chemical formula,  $M_nC_m$ .
- [23] Uchoa, B., Cabrera, G. G., Castro Neto, A. H., Nodal superconductivity in transition metal dichalcogenides, *Phys. Rev. B* **71**, 184509 (2005).

We thank F. Guinea, N. M. R. Peres, and S.-W. Tsai for many discussions and comments. This work was supported by NSF grant DMR-0343790. B. U. acknowledges CNPq, Brazil, for the support under the grant 201007/2005-3.